

Reconfigurable Intelligent Surface Phase Hopping for Ultra-Reliable Communications

Karl-Ludwig Besser, *Student Member, IEEE* and Eduard A. Jorswieck, *Fellow, IEEE*

Abstract

We introduce a phase hopping scheme for reconfigurable intelligent surfaces (RISs) in which the phases of the individual RIS elements are randomly varied with each transmitted symbol. This effectively converts slow fading into fast fading. We show how this can be leveraged to significantly improve the outage performance and even achieve an outage probability of zero at a positive data rate *without* channel state information (CSI) at the transmitter and RIS. Furthermore, the same result can be accomplished even if only two possible phase values are available. Since we do not require perfect CSI at the transmitter or RIS, the proposed scheme has no additional communication overhead for adjusting the phases. This enables robust ultra-reliable communications with a reduced effort for channel estimation.

Index Terms

Reconfigurable intelligent surfaces, Phase hopping, Zero-outage capacity, Outage probability, Ultra-reliable communications.

I. INTRODUCTION

Reconfigurable intelligent surfaces (RISs) have been considered widely as a promising enabling technology for the next generation of wireless communications to provide a higher throughput, a lower latency, a better reliability, and an improved security [2]–[4]. They can be used to shape the propagation of electromagnetic waves [5], [6], which can in turn be used to improve wireless data

Parts of this work are presented at the 2021 IEEE 22nd International Workshop on Signal Processing Advances in Wireless Communications (SPAWC) [1].

The authors are with the Institute of Communications Technology, Technische Universität Braunschweig, 38106 Braunschweig, Germany (email: {k.besser, e.jorswieck}@tu-bs.de).

The work of K.-L. Besser is supported in part by the German Research Foundation (DFG) under grant JO 801/23-1.

transmission. A possible use case is the compensation of Doppler effects, e.g., in high-mobility scenarios [7], [8]. Further applications could include localization and sensing [9], [10].

The main focus in the aforementioned cases lies on the correct adjustment of the phase shifts of the individual RIS elements. Based on the direct channel as well as the RIS-assisted channel, [11] minimizes the total transmit power at the transmitter by jointly optimizing the transmit beamforming by an active antenna array at the transmitter and reflect beamforming by passive phase shifters at the RIS. A similar problem is considered in [12]. An optimization algorithm for finding the optimal RIS phases that maximize the energy efficiency in a multi-user downlink communication scenario is presented in [13]. The maximization of the weighted signal-to-interference-plus-noise ratio (SINR) in a two-user downlink network is considered in [14]. The optimal phase shifts for a maximum transmission rate of a single-antenna RIS-assisted communication system are derived in [15].

ScatterMIMO exploits smart surfaces to increase the scattering in the environment in order to provide multiple-input multiple-output (MIMO) spatial multiplexing gain and additional spatial diversity [16]. By a clever placement of the RIS, another virtual access point is created whose signals superimpose at the receiver.

However, the various optimization problems to find the optimal phase shifts typically require channel state information (CSI) at the RIS or transmitter. In contrast to this, we do not choose the RIS coefficients based on CSI and, thus, do not require CSI at the transmitter or at the RIS. Instead, we propose to use the RIS to *transform a slow-fading into a fast-fading channel*, in order to improve the reliability of the link. This is done by randomly varying the RIS phases with each transmitted symbol during a constant realization of the slow-fading channels. Due to some similarities to the well-known frequency hopping [17, Chap. 3], we call the proposed scheme *phase hopping* in the following. The idea stems from the following observation: depending on the antenna geometries, orientation and location of the transmitter, RIS, and receiver, we can be lucky and obtain a constructive superposition and achieve high data rate or we can be unlucky to get a destructive superposition and an outage. For ultra-reliable communications it is better to *sacrifice very high peak data rates to gain reliability and compensate poor data rates* by averaging over all possible fading states. Specifically, with the transformation to fast-fading, we can achieve a positive zero-outage capacity (ZOC). This is remarkable because usually CSI at the transmitter is required for this.

Our proposed transmission scheme is based on two different time-scales, which has been

considered in a similar way in previous works [8], [18]–[20]. In [8], a two-stage protocol is proposed to mitigate the Doppler effect in a high-mobility scenario. The protocol includes a training phase in order to adjust the RIS phases. In [18], the optimization of the RIS phases is split into a long-term optimization problem based on statistical CSI and a short-term optimization based on the faster varying instantaneous CSI. Similar ideas of leveraging long-term statistical CSI are used in [19], [20]. However, these previous works again focus on calculating and setting optimal RIS phases based on CSI. If they need to be set to particular values, there is a communication overhead to first estimate the channels, second compute the optimal phases, and third pass them to the RIS. In contrast, this is not necessary in our proposed phase hopping scheme.

In the research of metamaterials several different ideas are proposed on how elements that are capable of phase tuning can be designed [21]. There also exist prototypes of RIS elements with both continuous phase tuning [22], [23] and quantized phases, e.g., with down to only two available phase values [5], [24]. The influence of discrete phase shifts on the performance of communication systems has also been investigated in [25]–[27]. For this reason, we additionally investigate the performance of phase hopping under the assumption that only a finite set of possible RIS phases is available.

The contributions of this work are summarized as follows.

- We analyze the outage probability in a slow-fading RIS-assisted communication system without CSI at transmitter and RIS when the RIS phases are fixed to constant values. (Section III)
- We present a phase hopping communication scheme in which the phases of the RIS elements are randomly varied. It is shown that this significantly improves the ε -outage capacity for small ε . In particular, we show that a positive ZOC can be achieved by this scheme. (Section IV)
- Furthermore, it is shown that the same ZOC can be achieved for a large number of RIS elements N , if only a finite set of possible phase values is available. This even includes the case of 1-bit phase quantization, i.e., the set of possible RIS phases is $\{0, \pi\}$. (Section V)
- For the considered model, we show that, even in the simplest case of $N = 2$ elements and only two possible phase choices, we can achieve a positive ZOC by employing the proposed phase hopping scheme. (Section VI)

All of the calculations and simulations are made publicly available in interactive notebooks at [28].

Notation: Vectors are written in boldface letters, e.g., \mathbf{x} . We use F_X and f_X for the probability distribution of random variable X and its density, respectively. The expectation is denoted by \mathbb{E} and the probability of an event by \Pr . The uniform distribution on the interval $[a, b]$ is denoted as $\mathcal{U}[a, b]$. The normal distribution with mean μ and variance σ^2 is written as $\mathcal{N}(\mu, \sigma^2)$. The unit step function is written as $\mathbb{1}(x)$. The real and complex numbers are denoted by \mathbb{R} and \mathbb{C} , respectively. Logarithms, if not stated otherwise, are assumed to be with respect to the natural base.

II. SYSTEM MODEL AND PROBLEM FORMULATION

Throughout this work, consider a slow-fading single-input single-output (SISO) communication system which is assisted by an RIS with N elements between the transmitter and receiver. The received signal $y \in \mathbb{C}$ is then given as

$$y = Hx + n, \quad (1)$$

where $x \in \mathbb{C}$ is the transmitted signal, $H \in \mathbb{C}$ the overall fading coefficient, and $n \in \mathbb{C}$ circularly-symmetric complex additive white Gaussian noise (AWGN). Since we assume an RIS-assisted communication, the channel fading H is given by [13]

$$H = h_{\text{LOS}} + \mathbf{h}\Theta\mathbf{g}^T, \quad (2)$$

where $h_{\text{LOS}} \in \mathbb{C}$ is the channel coefficient of the line-of-sight (LOS) connection and $\mathbf{h} \in \mathbb{C}^{1 \times N}$ and $\mathbf{g} \in \mathbb{C}^{1 \times N}$ represent the channels from transmitter to RIS and from RIS to the receiver, respectively. The matrix $\Theta \in \mathbb{C}^{N \times N}$ is a diagonal matrix with the RIS phases on the main diagonal, i.e., $\Theta = \text{diag}(\exp(j\theta_1), \dots, \exp(j\theta_N))$. An illustration of the setup is given in Fig. 1.

This type of SISO model can originate from an RIS-aided mmWave MIMO link (similar to e.g. [29]) where the transmit beamforming and receive beamforming are both included in the effective channel vectors \mathbf{h} and \mathbf{g} , respectively. The RIS is located in the far-field of the transmitter and receiver. Therefore, we assume that both h_i and g_i are independent quasi-static fading coefficients with absolute value 1 and identically uniformly distributed phases, i.e., $h_i = \exp(j\varphi_i)$ and $g_i = \exp(j\psi_i)$ with $\varphi_i, \psi_i \sim \mathcal{U}[0, 2\pi]$. This is a special case of the fluctuating fading model [30]. The extension to a model with two path-losses for the transmitter-RIS and RIS-receiver links is straightforward.

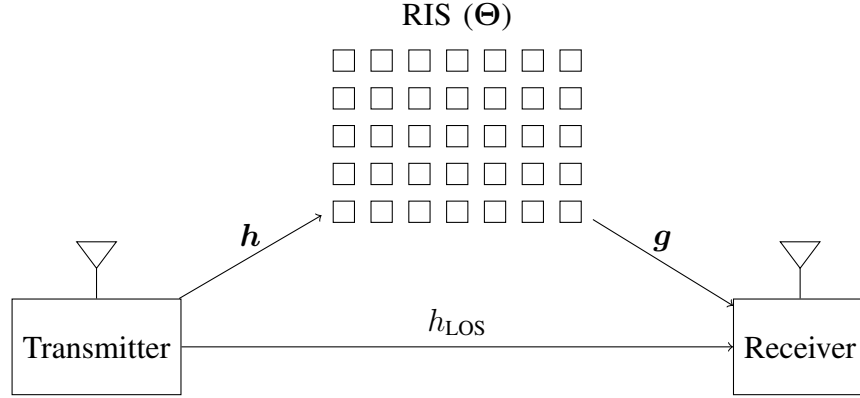


Figure 1. System model of the RIS-assisted communication system.

For the possible LOS component, we assume the same model as for the individual links in h and g . However, in order to reflect the signal-to-noise ratio (SNR) difference of the LOS component, it has an absolute value of a , i.e., we have that

$$h_{\text{LOS}} = a \exp(j\varphi_{\text{LOS}}). \quad (3)$$

Typically, we will have $a > 1$ in order to reflect a stronger LOS connection. It is straightforward to normalize the absolute values with respect to a , such that the non-line-of-sight (NLOS) components have an absolute value smaller than 1. However, for simplifying notation, we will use the above normalization throughout this work. Additionally, we will assume that a and φ_{LOS} have the same slow fading time-scale as ϕ_i and ψ_i .

Based on these assumptions, we can simplify the expression of H in (2) to

$$\begin{aligned} H &= h_{\text{LOS}} + \sum_{i=1}^N h_i [\Theta]_{ii} g_i \\ &= a \exp(j\varphi_{\text{LOS}}) + \sum_{i=1}^N \exp(j(\varphi_i + \psi_i + \theta_i)). \end{aligned} \quad (4)$$

In the case of perfect CSI at all communication parties, the RIS phases θ_i can be optimized based on the channel realizations φ_i and ψ_i [15]. However, while we assume that the receiver has perfect CSI about the channel realization of H , we assume that neither transmitter nor RIS have CSI. This implies that we do not need to estimate the component channels h_{LOS} , h , and g , but only the effective channel and only at the receiver side. At the transmitter, we, therefore, do not perform any power or rate adaption and assume a constant transmit power throughout this work.

The suitable performance metrics for this slow fading channel are the outage probability ε and the ε -outage capacity R^ε [31]. An outage occurs if the instantaneous channel capacity

$$C_{\text{inst}} = \log_2 (1 + |H|^2)$$

for a (constant) realization of the channels h_{LOS} , \mathbf{h} , and \mathbf{g} is less than the transmission rate R . The outage probability is, therefore, defined as

$$\varepsilon = \Pr (C_{\text{inst}} < R) . \quad (5)$$

The ε -outage rate is then defined as the maximum transmission rate for which the probability of an outage is at most ε [31],

$$R^\varepsilon = \sup_{R \geq 0} \left\{ R \mid \Pr (C_{\text{inst}} < R) \leq \varepsilon \right\} . \quad (6)$$

A. Problem Formulation

For the communication scenario described above, the following question arises. *What is a suitable technique to adjust the RIS phases (without perfect CSI) in order to achieve a high ε -outage capacity, especially for small ε , e.g., less than 10^{-3} ?*

In this work, we will answer this question by proposing a phase hopping technique in which the phases of the individual RIS elements are randomly changed for each transmitted symbol. For comparison, we will first investigate the simple approach of fixing all RIS phases in the following section.

III. STATIC RIS PHASES

Since we do not have any CSI at the transmitter or at the RIS, there are multiple ways of setting the phases of the individual RIS elements. A straightforward way would be to fix each phase to a constant value θ_i . Without loss of generality, we assume that $\theta_i = 0$ for all $i = 1, \dots, N$.

This yields the effective channel for static RIS phases as

$$H_{\text{stat}} = h_{\text{LOS}} + \sum_{i=1}^N \exp(j\tilde{\varphi}_i) , \quad (7)$$

where we introduce the shorthand $\tilde{\varphi}_i = \varphi_i + \psi_i \pmod{2\pi}$.

The instantaneous channel capacity is then given as

$$C_{\text{inst,stat}} = \log_2 (1 + |H_{\text{stat}}|^2) . \quad (8)$$

A. Non-Line-of-Sight Scenario

For simplicity, we first consider the NLOS scenario, i.e., $h_{\text{LOS}} = 0$. In this case, the outage probability is given in the following theorem.

Theorem 1 (Outage Probability NLOS with Static Phases). *Consider the previously described RIS-assisted slow fading communication scenario without CSI at the transmitter and RIS. There is no LOS connection, i.e., $h_{\text{LOS}} = 0$. The phases of the N RIS elements θ_i are fixed to constant values. The outage probability is then exactly given by*

$$\varepsilon_{\text{stat,NLOS}} = \sqrt{2^R - 1} \int_0^{\infty} J_1(\sqrt{2^R - 1} \cdot t) J_0(t)^N dt. \quad (9)$$

For large N , it can be approximated by

$$\varepsilon_{\text{stat,NLOS}} \approx 1 - \exp\left(-\frac{2^R - 1}{N}\right). \quad (10)$$

Proof. It follows from (5) and (8) that the outage probability ε is given in this case as

$$\varepsilon_{\text{stat,NLOS}} = \Pr\left(\left|\sum_{i=1}^N \exp(j\tilde{\varphi}_i)\right|^2 < 2^R - 1\right) \quad (11)$$

for a given transmission rate R . Since $\tilde{\varphi}_i$ are independent and identically distributed (i.i.d.) with an uniform distribution over $[0, 2\pi]$, we can determine the cumulative distribution function (CDF) of

$$S_N = \left|\sum_{i=1}^N \exp(j\tilde{\varphi}_i)\right|,$$

as [32, Sec. 3.2.1]

$$F_{S_N}(s) = s \int_0^{\infty} J_1(s \cdot t) J_0(t)^N dt. \quad (12)$$

The functions J_0 and J_1 are the Bessel functions of the first kind of orders zero and one, respectively. With (12), we can rewrite $\varepsilon_{\text{stat,NLOS}}$ as

$$\begin{aligned} \varepsilon_{\text{stat,NLOS}} &= F_{S_N}\left(\sqrt{2^R - 1}\right) \\ &= \sqrt{2^R - 1} \int_0^{\infty} J_1(\sqrt{2^R - 1} \cdot t) J_0(t)^N dt, \end{aligned}$$

which gives the first statement of the theorem.

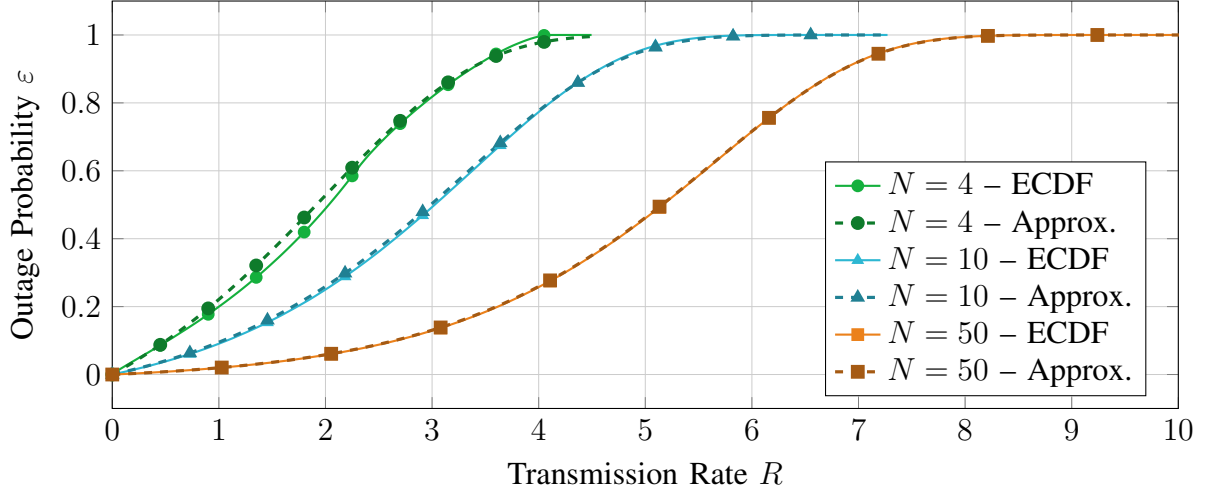


Figure 2. Outage probability for an RIS with N elements with constant phases. The solid lines show the ECDF obtained by Monte Carlo simulations. For comparison, the dashed lines indicate the approximation for large N from (10).

Since the evaluation of (9) can be quite tedious for general N , we will use the limit distribution for large N as an approximation, which is given by a Rayleigh distribution [32, Sec. 3.4.1]

$$\lim_{N \rightarrow \infty} F_{S_N}(s) = 1 - \exp\left(-\frac{s^2}{N}\right), \quad (13)$$

yielding

$$\varepsilon_{\text{stat,NLOS}} \approx 1 - \exp\left(-\frac{2^R - 1}{N}\right),$$

which concludes the proof. \square

In Fig. 2, we show the outage probability $\varepsilon_{\text{stat,NLOS}}$ for an RIS-assisted communication with static phases and no LOS connection. The results are shown for RISs with $N = 4$, $N = 10$, and $N = 50$ elements. The solid lines are the empirical distribution functions (ECDFs) obtained by Monte Carlo (MC) simulations with 10^6 samples. For comparison, the approximation from (10) is shown. The source code to reproduce all results can be found at [28]. From the figure, it can be observed that the approximation for large N is already accurate for $N \geq 10$. Furthermore, the ε -outage capacity is increasing with increasing N . However, the typical outage probability requirement for modern wireless systems lies between 10^{-3} and 10^{-9} depending on the application. The corresponding supported data rate is very low. Additionally, the *zero*-outage capacity is zero in all cases.

Remark 1. The ε -outage capacity R^ε in general can be determined from R in (10) as

$$R^\varepsilon = \log_2(1 - N \log(1 - \varepsilon)) . \quad (14)$$

From (14), it can be seen that the ZOC R^0 is zero for all N when the RIS phases are set to constant values.

B. Line-of-Sight Scenario

We now assume that there exists an additional LOS connection between the transmitter and receiver, which is given by

$$h_{\text{LOS}} = a \exp(j\varphi_{\text{LOS}}) , \quad (15)$$

where $a > 0$ denotes the absolute value and $\varphi_{\text{LOS}} \sim \mathcal{U}[0, 2\pi]$ describes the slow-fading phase of the LOS connection. Additionally, we assume that φ_{LOS} is independent of $\tilde{\varphi}_i$. The outage probability for this scenario is stated in the following theorem.

Theorem 2 (Outage Probability LOS with Static Phases). *Consider the previously described RIS-assisted slow fading communication scenario without CSI at the transmitter and RIS. There exists a LOS connection with absolute value a between transmitter and receiver. The phases of the N RIS elements θ_i are fixed to constant values. The outage probability for this scenario can be approximated as*

$$\varepsilon_{\text{stat,LOS}} \approx 1 - Q_1 \left(\sqrt{\frac{2a^2}{N}}, \sqrt{\frac{2}{N}(2^R - 1)} \right) , \quad (16)$$

where $Q_M(a, b)$ denotes the Marcum Q -function [33].

Proof. As we have seen in the above results for the NLOS case, it can be infeasible to calculate the exact expression of the distribution of the channel H . We will therefore focus on the approximation for large N in the following.

By the central limit theorem, we obtain the approximation that for large N [32, Chap. 3.4]

$$\sum_{i=1}^N \exp(j\tilde{\varphi}_i) = N\bar{C} + jN\bar{I} \quad (17)$$

with independent \bar{C} and \bar{I} , which are normally distributed according to $\bar{C}, \bar{I} \sim \mathcal{N}(0, \frac{1}{2N})$. This yields the following approximation for H_{stat}

$$H_{\text{stat}} = (a \cos \varphi_{\text{LOS}} + N\bar{C}) + j(a \sin \varphi_{\text{LOS}} + N\bar{I}) \quad (18)$$

$$= N \left(\hat{C} + j\hat{I} \right) , \quad (19)$$

with

$$\hat{C} \sim \mathcal{N}\left(\frac{a \cos \varphi_{\text{LOS}}}{N}, \frac{1}{2N}\right) \quad \text{and} \quad \hat{I} \sim \mathcal{N}\left(\frac{a \sin \varphi_{\text{LOS}}}{N}, \frac{1}{2N}\right).$$

With this, we can derive that

$$Z = \frac{2|H_{\text{stat}}|^2}{N} = 2N(\hat{C}^2 + \hat{I}^2) \quad (20)$$

is distributed according to a noncentral χ^2 distribution with 2 degrees of freedom and noncentrality parameter $\frac{2a^2}{N}$, i.e., $Z \sim \chi^2\left(2, \frac{2a^2}{N}\right)$ [34, Chap. 12].

We can now determine the outage probability according to (5) for the case of static RIS phases with an LOS connection as

$$\begin{aligned} \varepsilon_{\text{stat,LOS}} &= F_Z\left(\frac{2}{N}(2^R - 1)\right) \\ &= 1 - Q_1\left(\sqrt{\frac{2a^2}{N}}, \sqrt{\frac{2}{N}(2^R - 1)}\right), \end{aligned}$$

where $Q_M(a, b)$ denotes the Marcum Q-function [33], which concludes the proof. \square

Corollary 1. *In the considered communication scenario, the approximated outage probability $\varepsilon_{\text{stat,LOS}}$ from (16) in the LOS case is not greater than the approximated outage probability $\varepsilon_{\text{stat,NLOS}}$ from (10) in the NLOS case, i.e.,*

$$\varepsilon_{\text{stat,LOS}} \leq \varepsilon_{\text{stat,NLOS}}.$$

Proof. The proof can be found in Appendix A. \square

An example that illustrates this result can be found in Fig. 3. The outage probabilities $\varepsilon_{\text{stat,LOS}}$ are shown for $N = 4$, $N = 10$, and $N = 50$. The approximation from (16) is compared to simulation results obtained by MC simulations with 10^6 samples. The absolute value of the LOS component is set to $a = 2$. It can be seen that the approximation for large N is already quite accurate for $N = 4$. For comparison, we additionally show the outage probability of the NLOS scenario for $N = 50$. As expected from Corollary 1, it can be seen that the ε -outage capacity for LOS is greater than in the NLOS case, due to the additional LOS component. However, for small ε , the ε -outage capacity is still very small for all N .

Remark 2. From (16) it can be seen that the ε -outage capacity can be determined using the quantile function of a non-central χ^2 -distribution. It follows that the ZOC is zero for all N , just as in the NLOS case.

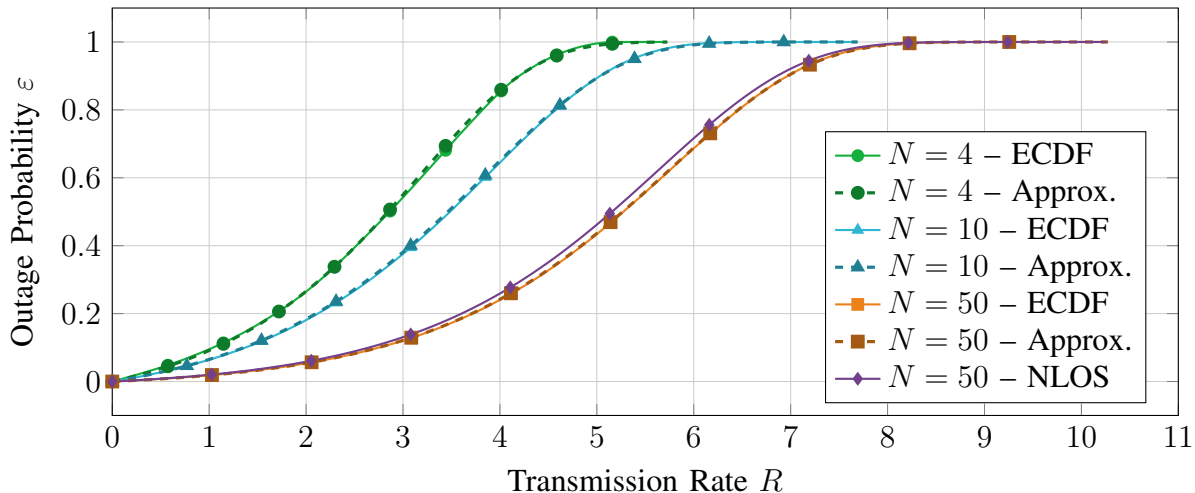


Figure 3. Outage probability for a LOS scenario with an RIS with N elements. The RIS phases are fixed. The strength of the LOS connection is $a = 2$. The solid lines show the ECDF obtained by Monte Carlo simulations. For comparison, the dashed lines indicate the approximation for large N from (16). For $N = 50$, the outage probability of the NLOS scenario is additionally given.

IV. RANDOMLY VARYING PHASES

After analyzing the outage probability when fixing all RIS phases, we will now introduce a new *phase hopping* scheme which significantly improves the ε -outage capacity of the overall communication system for small tolerated outage probabilities ε . We summarize the scheme in the following definition.

Definition 1 (RIS Phase Hopping Scheme). In the *RIS phase hopping* scheme, the phases θ_i , $i = 1, \dots, N$, of the N RIS elements are randomly varied with each transmitted symbol. The phase sequence is determined by a pseudo-random sequence which is known at all parties in the communication system.

Instead of fixing the phases θ_i of the RIS elements, they are varied randomly at each transmitted symbol. Since this changing is extremely fast compared to the time-scale of the slow-fading channels, it creates an artificial fast-fading. However, the phases are adjusted by an underlying pseudo-random sequence that is known at all communication parties, and thus, we obtain perfect CSI of the fast-fading channel at the receiver. With this perfect channel-state information at the receiver (CSI-R) of the fading realizations (including the artificial fast fading), we can apply the well-known results for the ergodic capacity, which can be achieved by averaging over the

received symbols during one constant (slow-fading) realization of the channels h_{LOS} , \mathbf{h} and \mathbf{g} . The ergodic capacity is then given by [31]

$$C_{\text{erg}} = \mathbb{E}_{\boldsymbol{\theta}} \left[\log_2 \left(1 + \left| h_{\text{LOS}} + \sum_{i=1}^N \exp(j(\theta_i + \tilde{\varphi}_i)) \right|^2 \right) \right], \quad (21)$$

where we again set $\tilde{\varphi}_i = \varphi_i + \psi_i \bmod 2\pi$ as the overall phase of the constant channels \mathbf{h} and \mathbf{g} .

It directly follows, that an outage according to (5) only occurs, if the transmission rate R is larger than the ergodic capacity,

$$\varepsilon_{\text{var}} = \Pr(C_{\text{erg}} < R). \quad (22)$$

Throughout this section, we will assume that the RIS phases θ_i are independently and uniformly distributed over $[0, 2\pi]$. If we had perfect CSI at the RIS, the phases θ_i could be adjusted optimally such that they compensate the phase shifts $\tilde{\varphi}_i$ of the channels, i.e., $\theta_i = -\tilde{\varphi}_i$ [15].

Remark 3 (Connection to Frequency-Hopping). The presented idea of *RIS phase hopping* is closely related to the well-established frequency-hopping method [17, Chap. 3]. In frequency-hopping, the carrier frequency is frequently changed in order to avoid interference that might occur on specific frequencies. It, therefore, helps to also increase the reliability of the transmission. Our proposed phase hopping scheme has the following parallels to frequency-hopping. In our case, the hop set consists of the possible phase values of the RIS elements. The hop rate is set to match the symbol rate, i.e., we change the phases with each transmitted symbol. Just like in frequency-hopping systems, we assume that all users know the hop pattern based on a pseudo-random phase sequence [35].

Remark 4 (Deterministic Hop Sequence for Finitely Many Symbols). The ergodic capacity from (21) is an asymptotic performance metric based on an infinite number of transmitted symbol. Therefore, the immediate question arises, if the proposed scheme can still be used for a finite number of fast-changing RIS phases. In particular, we are interested in achieving a positive ZOC. This is possible by repeating each transmitted symbol twice and setting the RIS phases according to a deterministic sequence. A detailed analysis can be found in Appendix B.

A. Non-Line-of-Sight Scenario

We will again start with the simpler NLOS scenario, where $h_{\text{LOS}} = 0$. The outage probability for this scenario can be found in the following theorem.

Theorem 3 (Outage Probability NLOS with Phase Hopping). *Consider the previously described RIS-assisted slow fading communication scenario without CSI at the transmitter and RIS. There is no LOS connection, i.e., $h_{LOS} = 0$. The RIS applies phase hopping with i.i.d. and uniformly distributed θ_i . The outage probability is then given by*

$$\varepsilon_{var,NLOS} = \mathbb{1} (R - C_{erg,NLOS}) , \quad (23)$$

with

$$C_{erg,NLOS} = \int_0^N \log_2 (1 + s^2) \int_0^\infty st J_0(st) J_0(t)^N dt ds . \quad (24)$$

Proof. For i.i.d. θ_i with a uniform distribution on $[0, 2\pi]$, the exact CDF of $\left| \sum_{i=1}^N \exp(j(\tilde{\varphi}_i + \theta_i)) \right|$ is given according to (12). The probability density function (PDF) f_{S_N} is given by [32, Eq. (3.2.3)]

$$f_{S_N}(s) = \int_0^\infty st J_0(st) J_0(t)^N dt, \quad 0 \leq s \leq N . \quad (25)$$

Combining this with the expectation from (21) yields the expression in (24). Note that this ergodic capacity is independent of the realizations of \mathbf{g} and \mathbf{h} . Thus, the outage probability from (22) is a step function as given in (23). \square

Even though the expression for the ergodic capacity in (24) looks cumbersome, it can be efficiently calculated numerically. For this, we need the following observation. The Hankel transform of order ν of function f is defined as [36, Chap. 9]

$$\mathcal{H}_\nu\{f(t)\}(s) = \int_0^\infty f(t) J_\nu(st) t dt . \quad (26)$$

With this, we can rewrite (24) in terms of the Hankel transform of $J_0(t)^N$ as

$$C_{erg,NLOS} = \int_0^N \log_2 (1 + s^2) s \mathcal{H}_0 \{ J_0(t)^N \}(s) ds . \quad (27)$$

This can then be efficiently calculated numerically [37]. For the results presented in the following, we use the implementation in the `hankel` library [38] in Python. The source code to reproduce all calculations and simulations can be found in [28].

However, this method still requires a specialized implementation of the Hankel transform, which might not be widely available. We, therefore, present the following approximation for large N , which is easier to evaluate and useful as a guideline for system design.

Theorem 4 (Approximate Outage Probability NLOS with Phase Hopping). *Consider the previously described RIS-assisted slow fading communication scenario without CSI at the transmitter and*

RIS. There is no LOS connection, i.e., $h_{LOS} = 0$. The RIS applies phase hopping with i.i.d. and uniformly distributed θ_i . The outage probability is then approximated by

$$\varepsilon_{var,NLOS} \approx \mathbb{1} \left(R + \frac{\exp\left(\frac{1}{N}\right) \text{Ei}\left(-\frac{1}{N}\right)}{\log 2} \right). \quad (28)$$

Proof. For independent θ_i and with the approximation for large N from (13), we have that $\left| \sum_{i=1}^N \exp(j(\tilde{\varphi}_i + \theta_i)) \right|^2$ is exponentially distributed with mean N . For this case, the ergodic capacity from (21) is calculated as

$$C_{\text{erg,NLOS}} = \mathbb{E}_{S^2 \sim \exp(1/N)} [\log_2(1 + S^2)] \quad (29)$$

$$= -\frac{\exp\left(\frac{1}{N}\right) \text{Ei}\left(-\frac{1}{N}\right)}{\log 2}, \quad (30)$$

with Ei being the exponential integral [39, Sec. 5.1].

It is straightforward to see that the ergodic capacity in (30) is independent of the realization of $\tilde{\varphi}_i$, since it only provides a constant offset for θ_i . The outage probability from (5) will therefore be 0, if a rate R less than the ergodic capacity $C_{\text{erg,NLOS}}$ is used for transmission and 1 otherwise, i.e.,

$$\varepsilon_{\text{var,NLOS}} = \mathbb{1} \left(R + \frac{\exp\left(\frac{1}{N}\right) \text{Ei}\left(-\frac{1}{N}\right)}{\log 2} \right) = \begin{cases} 0 & R \leq C_{\text{erg,NLOS}} \\ 1 & \text{otherwise.} \end{cases}$$

□

First, we want to verify how accurate the approximation in Theorem 4 is. In Fig. 4, we show the exact ergodic capacity from (27) together with the approximation for large N from (30). As expected, it can be seen that the approximation becomes more accurate with increasing N . At $N = 6$, the difference between exact and approximate value is around 0.035 which corresponds to a relative error of around 1.5%. In contrast, at $N = 50$, the difference is only around 0.0064, which is a relative error of around 0.13%. Overall, it can be observed in that the approximation from (30) is less than the exact value, i.e., it is a lower bound¹. It can, therefore, serve as a worst case design guideline, which is particularly useful for ultra-reliable communication systems.

The results in Theorems 3 and 4 imply that the ε -outage capacity is concentrated on a single value $C_{\text{erg,NLOS}}$. This also includes the *zero*-outage capacity and it immediately follows that

¹We conjecture that this observation holds true in general for all N . Unfortunately, we were not able to prove this rigorously at this point.

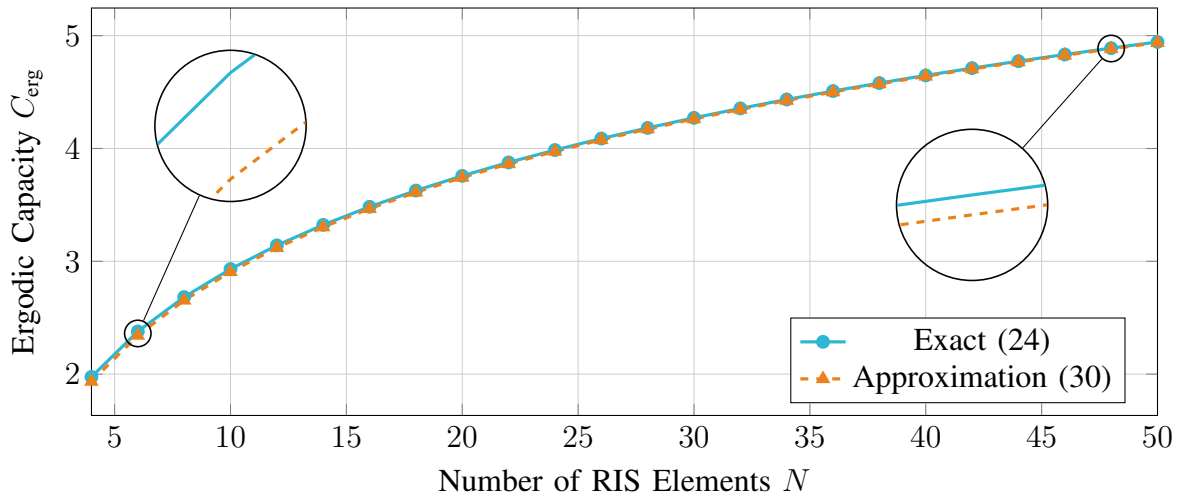


Figure 4. Comparison of the exact and approximate ergodic capacities from (24) and (30), respectively, for an NLOS communication system with phase hopping.

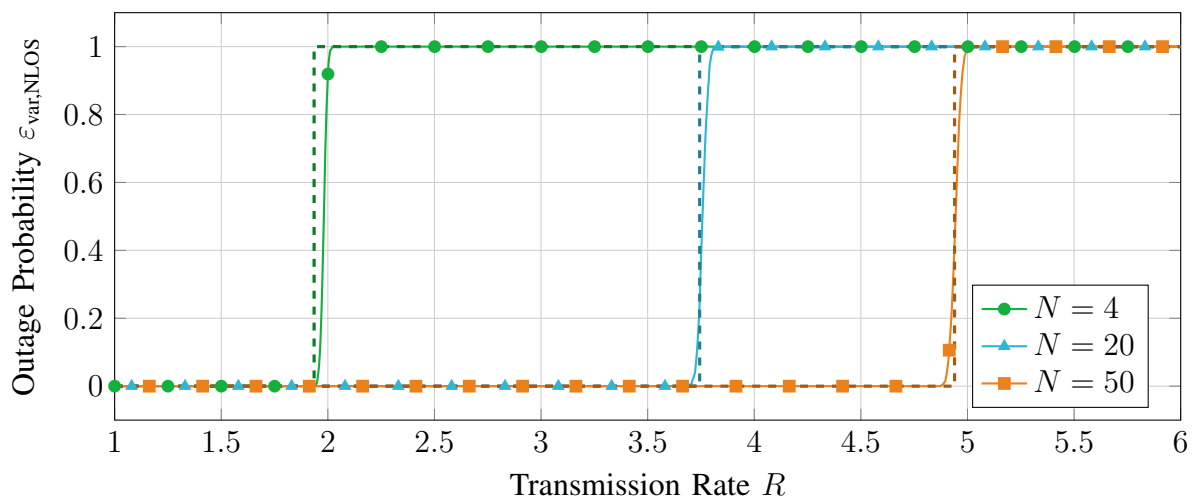


Figure 5. Outage probability for an NLOS scenario. The phases of the RIS with N elements are randomly varied. The solid lines show the ECDF obtained by Monte Carlo simulations. For comparison, the dashed lines indicate the approximation for large N from (28).

we can achieve a positive ZOC by constantly changing the N RIS phases independently. This is an interesting phenomenon since the ZOC is zero for the typically considered slow-fading channels with independent fading and constant transmit power, e.g., multi-antenna systems with independent Rayleigh fading [40].

The outage probability $\epsilon_{\text{var,NLOS}}$ is exemplarily shown in Fig. 5 for $N = 4$, $N = 20$, and

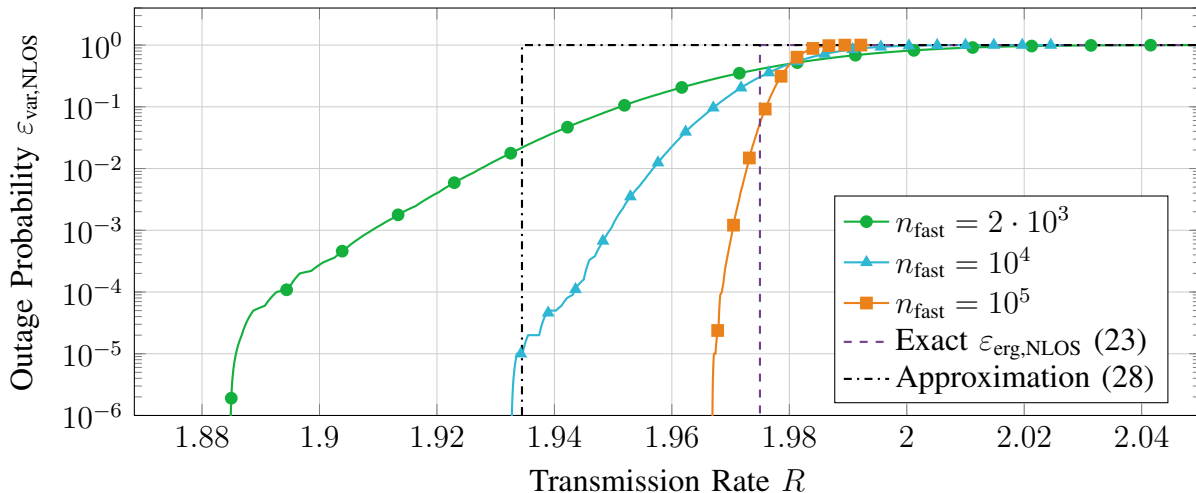


Figure 6. Outage probability for an NLOS scenario. The RIS with $N = 4$ elements employs phase hopping. The solid lines show the ECDF obtained by Monte Carlo simulations with 10^5 slow fading realizations and n_{fast} fast fading realizations. For comparison, the dashed line indicates the exact outage probability from (23) and the dash-dotted line indicates the approximation for large N from (28).

$N = 50$. Besides the approximation from (28), we show results obtained from MC simulations with 1000 slow-fading realizations of \mathbf{h} and \mathbf{g} , each containing 5000 fast-fading realizations of $\boldsymbol{\theta}$. The source code to reproduce the figure can be found in [28]. First, the step-like behavior can immediately be seen from Fig. 5. This directly shows the significant improvement in terms of the ε -outage capacity for small ε . However, due to the averaging over a finite number of symbols, the outage probability does not behave like a perfect step function. By the central limit theorem, this sampling distribution of the mean can be approximated by a Gaussian distribution.

In Fig. 6, we show the simulated outage probability for different numbers of fast fading samples n_{fast} , over which the average is calculated. This is done for 10^5 slow fading realizations. The number of RIS elements is set to $N = 4$ and both the exact outage probability from (23) and the approximation from (28) are presented for comparison. First, it can be observed that the simulated outage probability approaches the exact one for an increasing number of phase hopping symbols n_{fast} . Next, even when only averaging over 10^4 symbols, the ε -outage rate for $\varepsilon = 10^{-3}$ is around 1.95, which lies between the approximation (1.934) and the exact value (1.975).

B. Line-of-Sight Scenario

If we have an additional LOS component, the efficient channel is given as

$$H_{\text{var}} = a \exp(j\varphi_{\text{LOS}}) + \sum_{i=1}^N \exp(j(\tilde{\varphi}_i + \theta_i)), \quad (31)$$

where $a > 0$ is the fixed absolute value of the LOS component and $\varphi_{\text{LOS}} \sim \mathcal{U}[0, 2\pi]$ its slow-fading phase.

Theorem 5 (Outage Probability LOS with Phase Hopping). *Consider the previously described RIS-assisted slow fading communication scenario without CSI at the transmitter and RIS. There exists a LOS connection with absolute value a between transmitter and receiver. The RIS applies phase hopping with i.i.d. and uniformly distributed θ_i . The outage probability for this scenario can be approximated as*

$$\varepsilon_{\text{var,LOS}} = \mathbb{1}(R - C_{\text{erg,LOS}}), \quad (32)$$

with

$$C_{\text{erg,LOS}} = \int_0^\infty \frac{1}{N} \log_2(1 + s) \exp\left(\frac{-(a^2 + s)}{N}\right) I_0\left(\frac{2a}{N}\sqrt{s}\right) ds, \quad (33)$$

and I_0 being the modified Bessel function of the first kind and order zero [39, Eq. 9.6.16].

Proof. Similarly to case of static RIS phases, we will use an approximation of the channel coefficient H_{var} for large N in the following. Adapting the steps from Section III-B, we again get that

$$Z = \frac{2|H_{\text{var}}^2|}{N} \quad (34)$$

is distributed according to a noncentral χ^2 distribution with 2 degrees of freedom and noncentrality parameter $\frac{2a^2}{N}$.

From this, we can derive the PDF of $|H_{\text{var}}|^2$ as

$$f_{|H|^2}(s) = \frac{1}{N} \exp\left(\frac{-(a^2 + s)}{N}\right) I_0\left(\frac{2a}{N}\sqrt{s}\right), \quad (35)$$

where I_0 denotes the modified Bessel function of the first kind and order zero [39, Eq. 9.6.16].

The ergodic capacity is then calculated as

$$\begin{aligned} C_{\text{erg,LOS}} &= \mathbb{E} [\log_2(1 + |H_{\text{var}}|^2)] \\ &= \int_0^\infty \frac{1}{N} \log_2(1 + s) \exp\left(\frac{-(a^2 + s)}{N}\right) I_0\left(\frac{2a}{N}\sqrt{s}\right) ds. \end{aligned}$$

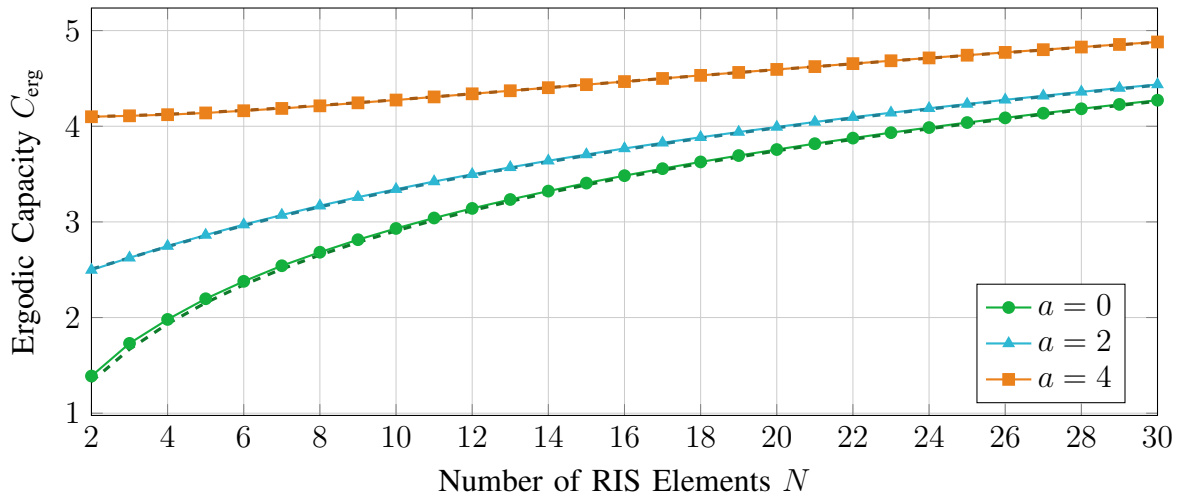


Figure 7. Ergodic capacity for an LOS scenario. The phases of the RIS with N elements are randomly varied. The solid lines show the ECDF obtained by Monte Carlo simulations. For comparison, the dashed lines indicate the approximation for large N from (33).

It is clear to see that this ergodic capacity does not depend on the realizations of h_{LOS} , \mathbf{h} , and \mathbf{g} . Thus, the outage probability according to (22) is again a step function

$$\varepsilon_{\text{var,LOS}} = \mathbb{1}(R - C_{\text{erg,LOS}}), \quad (36)$$

which concludes the proof. \square

The ergodic capacity in (33) has no known closed-form expression, however, it can be efficiently calculated numerically. This is used for the results that are presented in the following. The source code to reproduce the calculations and simulations can be found in [28].

In Fig. 7, the ergodic capacity $C_{\text{erg,LOS}}$ is shown for different values of the strength of the LOS connection a over the number of RIS elements N . The value $a = 0$ corresponds to the NLOS scenario. The solid lines show the results of the approximation for large N from (33). For comparison, the dashed lines indicate results of MC simulations with 1000 slow \times 5000 fast fading samples. First, it can be seen that the approximation for large N matches the simulation results accurately already for $N \geq 10$. As expected, the ergodic capacity increases with increasing a and also with increasing N . The increase in a is most prominent for small N and decreases with an increasing number of elements. This can also be seen from (33), since the influence of a becomes insignificant for very large N .

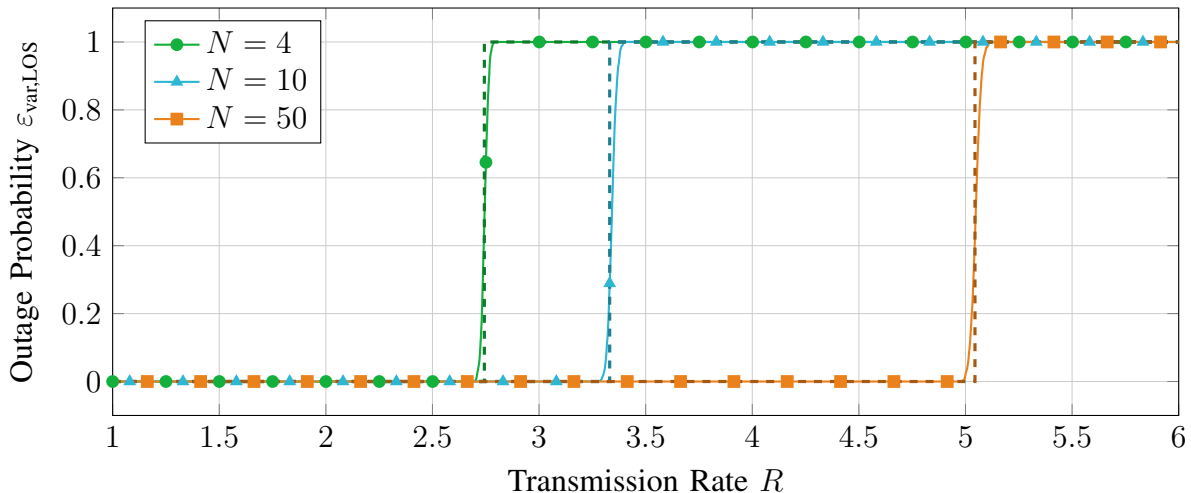


Figure 8. Outage probability for an LOS scenario with $a = 2$. The phases of the RIS with N elements are randomly varied. The solid lines show the ECDF obtained by Monte Carlo simulations. For comparison, the dashed lines indicate the approximation for large N from (32).

Next, we show the outage probability for $a = 2$ and different values of N in Fig. 8. The theoretical curves obtained by the approximation for large N from (32) are indicated by dashed lines. Recall that they are step functions with a step from 0 to 1 at $C_{\text{erg,LOS}}$. In contrast, the results obtained by MC simulations are no perfect step functions. However, it can be seen that they are close to the approximation, even at a small value of $N = 4$. Most importantly, the outage probability in the simulations was zero for rates less than around 2.696 ($N = 4$). For comparison, the theoretical ZOC is around 2.742. A similar behavior can be observed for the larger values of N .

V. QUANTIZED PHASES

In the previous section, we analyzed the outage performance of an RIS-assisted communication system where the phases of the individual RIS elements could be set to arbitrary values. However, in practice this might not be possible and only a discrete set of phase values may be available.

As in Section IV, we assume that the phases θ_i of the N RIS elements change with each transmitted symbol. However, the values of θ_i are now from a discrete set of phases \mathcal{Q} , i.e., we have

$$\theta_i \in \mathcal{Q} = \left\{ k \frac{2\pi}{K} \mid k = 0, \dots, K - 1 \right\}, \quad i = 1, \dots, N, \quad (37)$$

where K is the number of quantization steps.

The expected value in the ergodic capacity expression from (21) is then simply a weighted sum

$$C_{\text{erg}} = \sum_{\boldsymbol{\theta} \in \mathcal{Q}^N} \Pr(\boldsymbol{\theta}) \log_2 \left(1 + \left| h_{\text{LOS}} + \sum_{i=1}^N \exp(j(\tilde{\varphi}_i + \theta_i)) \right|^2 \right). \quad (38)$$

Evaluating this expression exactly can be cumbersome for general K and N , since it involves calculating all combinations of phases. Fortunately, for sufficiently large N , we can apply the central limit theorem to obtain approximate results, which will be shown in the following.

Theorem 6 (Outage Probability with Phase Hopping and Quantized Phases). *Consider the previously described RIS-assisted slow fading communication scenario without CSI at the transmitter and RIS. There is a possible LOS connection with absolute value a between transmitter and receiver. The phases θ_i of the N RIS elements are from the finite set \mathcal{Q} as defined in (37). The RIS applies phase hopping with i.i.d. and uniformly distributed θ_i , i.e., $\theta_i \stackrel{iid}{\sim} \mathcal{U}(\mathcal{Q})$. For large N , the outage probability for this scenario can be approximated according to (32) for the LOS case. In the case of $a = 0$, i.e., a NLOS scenario, the outage probability is approximated by (28).*

Proof. First, we will only take a closer look at the NLOS part of H , i.e.,

$$\sum_{i=1}^N \exp(j(\tilde{\varphi}_i + \theta_i)).$$

We again assume that the phases θ_i are i.i.d. and uniformly distributed over \mathcal{Q} and randomly changing with each transmitted symbol. The phases $\tilde{\varphi}_i$ on the other hand are (continuously) uniformly distributed over $[0, 2\pi]$. The above expression can be equivalently expressed as

$$\sum_{i=1}^N \exp(j(\tilde{\varphi}_i + \theta_i)) = \sum_{i=1}^N \cos(\tilde{\varphi}_i + \theta_i) + j \sin(\tilde{\varphi}_i + \theta_i). \quad (39)$$

Due to the uniform quantization of the phases in \mathcal{Q} , we obtain

$$\mathbb{E}_{\theta_i \sim \mathcal{U}(\mathcal{Q})} [\cos(\tilde{\varphi}_i + \theta_i)] = \mathbb{E}_{\theta_i \sim \mathcal{U}(\mathcal{Q})} [\sin(\tilde{\varphi}_i + \theta_i)] = 0 \quad (40)$$

and

$$\text{var} [\cos(\tilde{\varphi}_i + \theta_i)] = \text{var} [\sin(\tilde{\varphi}_i + \theta_i)] = 0.5. \quad (41)$$

Note that it is crucial for the above to have the uniform quantization of the unit circle that we assumed for \mathcal{Q} in (37).

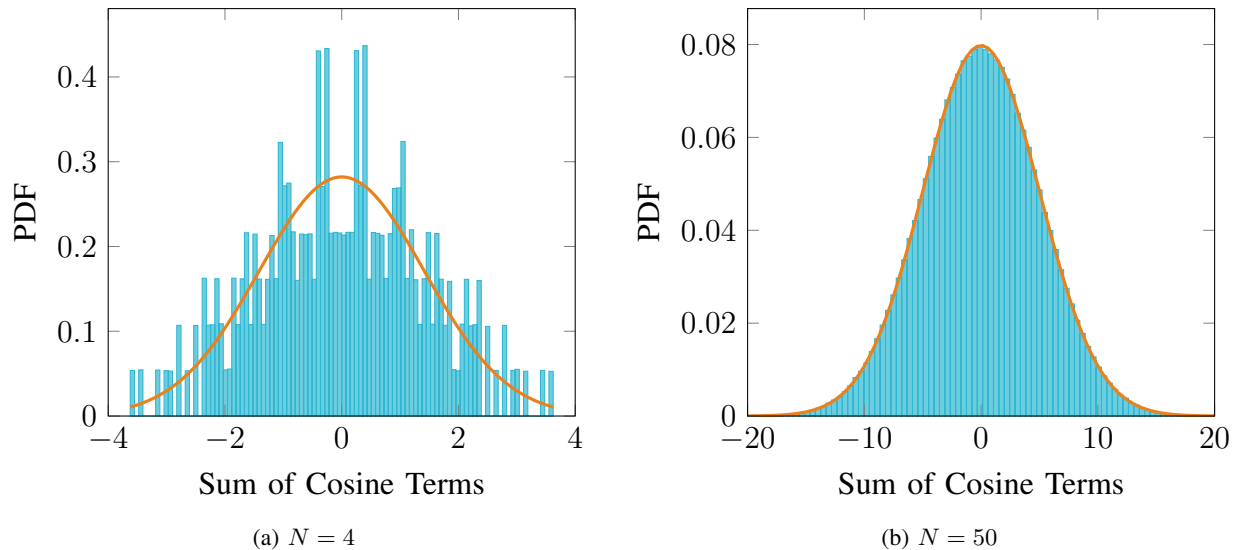


Figure 9. Histogram of $\sum_{i=1}^N \cos(\tilde{\varphi}_i + \theta_i)$ for two values of N and $K = 4$. The solid line indicates the PDF of the Gaussian approximation from (42).

Due to the independence, we can apply the central limit theorem for the sums, which yields for large N

$$\sum_{i=1}^N \cos(\tilde{\varphi}_i + \theta_i) \stackrel{N \rightarrow \infty}{\sim} \mathcal{N}\left(0, \frac{N}{2}\right). \quad (42)$$

The same holds for the sum $\sum_{i=1}^N \sin(\tilde{\varphi}_i + \theta_i)$. Note that this can be applied for any symmetric quantization of the phases, regardless of K .

A numerical validation of this observation is shown in Fig. 9. Histograms of $\sum_{i=1}^N \cos(\tilde{\varphi}_i + \theta_i)$ are presented for $N = 4$ in Fig. 9a and $N = 50$ in Fig. 9b. The number of phase quantization levels is set to $K = 4$. The values are obtained by MC simulations with 10^6 samples [28]. For comparison, the PDF of the approximate normal distribution from (42) is shown. It is clear to see that the approximation is accurate for $N = 50$. On the other hand, $N = 4$ is too small to use the normal distribution from (42) as an accurate approximation.

Now that we have established that both real and imaginary part of

$$\sum_{i=1}^N \exp(j(\tilde{\varphi}_i + \theta_i))$$

tend to normal distributions for large N , we can apply the results from Section IV-B. This means that

$$|H_{\text{quant}}|^2 = \left| h_{\text{LOS}} + \sum_{i=1}^N \exp(j(\tilde{\varphi}_i + \theta_i)) \right|^2$$

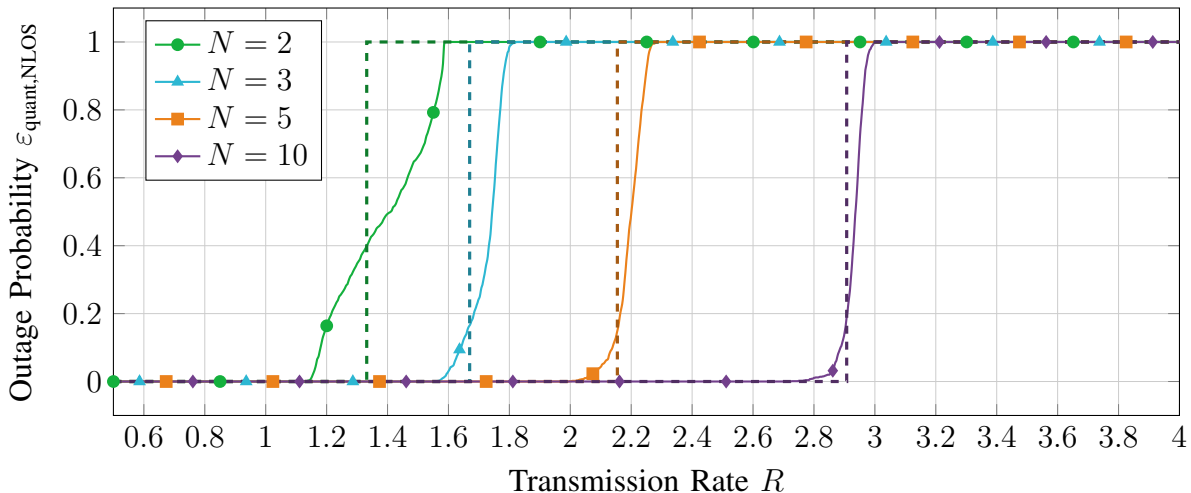


Figure 10. Outage probability for an NLOS scenario. The phases of the RIS with N elements are quantized with $K = 2$ steps, i.e., $\mathcal{Q} = \{0, \pi\}$. The phases are randomly and uniformly varied. The solid lines show the ECDF obtained by Monte Carlo simulations. The dashed lines indicate the approximation for large N .

is approximately distributed according to a non-central χ^2 distribution for sufficiently large N with the PDF from (35). The ergodic capacity is, therefore, also equal to the one of the non-quantized case from (33). It directly follows that the same holds for the NLOS case. \square

The important implication of Theorem 6 is that the outage probability for a phase hopping system with phase quantization is asymptotically equal to the case with continuous phases, independent of the number of quantization levels. For RIS with a large number of elements, we can therefore apply the results from the previous section as a design guideline, even if the RIS phases can only be set to a finite number of values.

In Fig. 10, we show the outage probability ε for an NLOS scenario and quantized phases for multiple numbers of RIS elements. The number of quantization levels is set to $K = 2$, i.e., the set of possible phase choices is $\mathcal{Q} = \{0, \pi\}$. The solid lines indicate the ECDFs obtained by MC simulations with $1000 \text{ slow} \times 5000 \text{ fast-fading}$ samples. For comparison, the dashed lines show the approximation for large N . As expected, the approximation as a step function gets more accurate with increasing N , even though only two possible phase values are available.

A different perspective of the results is given in Fig. 11, where we fix the number of RIS elements to $N = 2$ and vary the number of quantization levels K . It can be seen that the outage probability curves get closer to a step function with an increasing number of quantization levels.

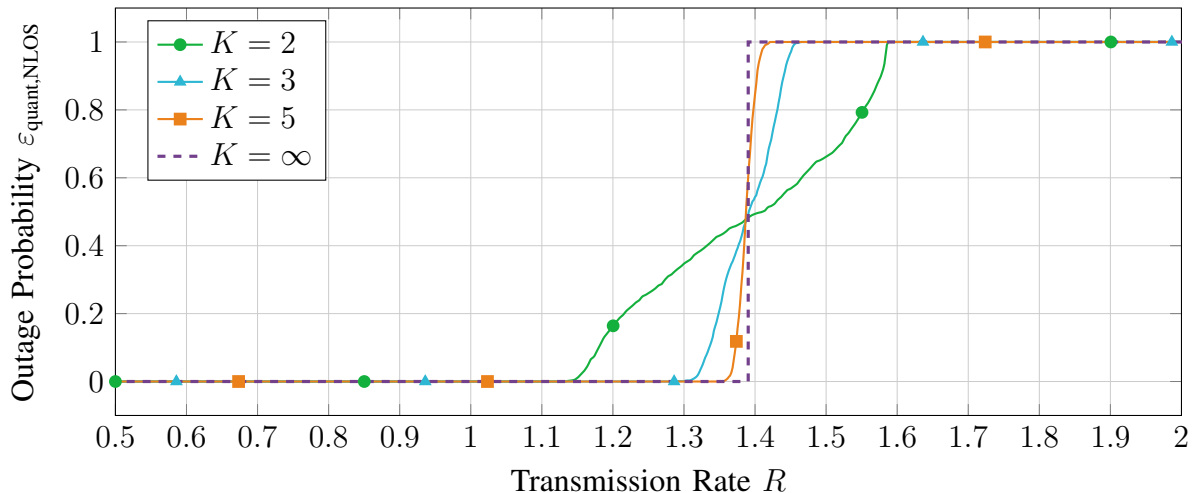


Figure 11. Outage probability for an NLOS scenario. The phases of the RIS with $N = 2$ elements are quantized with K steps and randomly varied. The solid lines show the ECDF obtained by Monte Carlo simulations. The dashed curve indicates the theoretical value without quantization from (23).

However, it should be noted that even in the case of $N = 2$ and $K = 2$, we obtain an ZOC of around 1.16 bits. This value will be quantified exactly in the following section.

Remark 5. It should be emphasized that the quantization does not change the ergodic capacity, and thus the ZOC, for sufficiently large N . This includes the one-bit-quantization $K = 2$, i.e., $\mathcal{Q} = \{0, \pi\}$, which can already be implemented with existing hardware [24]. Furthermore, this approximation is valid since we typically have RIS with $N > 50$ elements.

VI. OPTIMAL RIS PHASE DISTRIBUTION

Up to this point, we only considered varying the RIS independently and with an uniform distribution over the set $\mathcal{Q} \subseteq [0, 2\pi]$. However, since the system designer has full control over the way in which the individual RIS phases are varied, it is of interest to consider a more general problem formulation. In modern use cases, e.g., in the context of ultra-reliable low latency communication (URLLC), we are interested in maximizing the ε -outage capacity for very small ε . The extreme case is the *zero*-outage capacity. For a positive ZOC, we are able to transmit data over a slow fading channel without any outages and therefore without retransmissions. On the one hand this reduces the latency and on the other hand it saves energy by avoiding unnecessary transmissions.

Therefore, the natural question about the optimal joint distribution, that maximizes the ZOC, arises. For the NLOS scenario, this yields the following optimization problem over the joint distributions F_θ of the RIS phases $\theta_i \in \mathcal{Q}$

$$\max_{F_\theta} \min_{\tilde{\varphi}} \mathbb{E} \left[\log_2 \left(1 + \left| \sum_{i=1}^N \exp(j(\tilde{\varphi}_i + \theta_i)) \right|^2 \right) \right]. \quad (43)$$

A trivial upper bound is $\log_2(1 + N^2)$, which is attained for $\theta_i = -\tilde{\varphi}_i$ [15]. However, since we do not assume CSI at the transmitter or RIS, this is not a feasible solution in our considered scenario.

Since the optimization problem in (43) is non-trivial and a general solution is beyond the scope of this work, we focus on the specific example of a two-element RIS with two possible phase values, i.e., $N = 2$ and $K = 2$ in the following. For this particular example, we are able to solve the optimization problem in (43) for the best-possible distribution of the phases θ_1 and θ_2 and the resulting maximum ZOC.

Example (Two-Element RIS with Two Phases). Assuming a one bit quantization of the phase values yields the set of possible phase choices $\mathcal{Q} = \{0, \pi\}$. In the following, we use the notation $\Pr(\theta_1 = t_1, \theta_2 = t_2) = p(t_1, t_2)$ for the joint probability of the RIS phases and the equivalence

$$\left| e^{j(\tilde{\varphi}_1 + \theta_1)} + e^{j(\tilde{\varphi}_2 + \theta_2)} \right|^2 = 2 + 2 \cos(\Delta\tilde{\varphi} + \theta_1 - \theta_2),$$

with $\Delta\tilde{\varphi} = \tilde{\varphi}_1 - \tilde{\varphi}_2$. Combining this, we obtain the ergodic capacity from (38) for the case of $N = K = 2$ as

$$C_{\text{erg,qu}} = \log_2(3 + 2 \cos \Delta\tilde{\varphi}) (p(0, 0) + p(\pi, \pi)) + \log_2(3 - 2 \cos \Delta\tilde{\varphi}) (p(0, \pi) + p(\pi, 0)). \quad (44)$$

In order to derive the maximum ZOC according to the optimization problem (43), we first need to minimize $C_{\text{erg,qu}}$ with respect to $\Delta\tilde{\varphi}$. Using the standard approach by derivation, we obtain the following solution

$$\min_{\Delta\tilde{\varphi}} C_{\text{erg,qu}} = \begin{cases} A \log_2 5 & 0 \leq A < 0.5 \\ (1 - A) \log_2 5 & 0.5 \leq A \leq 1 \end{cases}, \quad (45)$$

with $A = p(0, 0) + p(\pi, \pi)$. The detailed discussions can be found at [28]. Next, we maximize (45) with respect to A , which yields the maximum ZOC as

$$\max_A \min_{\Delta\tilde{\varphi}} C_{\text{erg,qu}} = 0.5 \log_2 5, \quad (46)$$

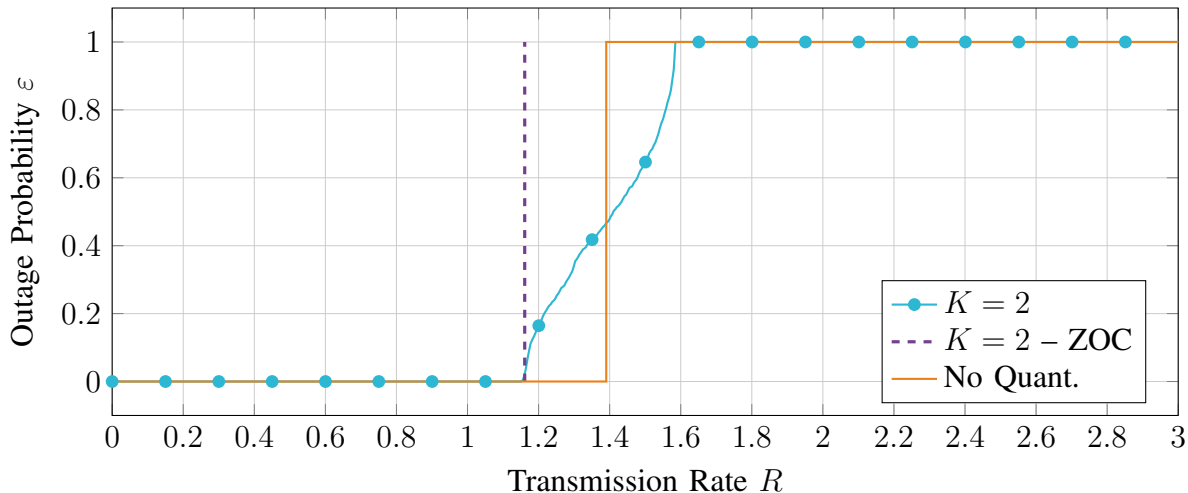


Figure 12. Outage probability for an RIS with $N = 2$ elements with varying phases. The phases are uniformly distributed over the set $\{0, \pi\}^2$. The dashed line indicates the theoretical ZOC from (46). The third curve gives a comparison to the case without phase quantization from (23).

at $A = 0.5$. This result indicates that all joint distributions of (θ_1, θ_2) , for which $p(0, 0) + p(\pi, \pi) = p(0, \pi) + p(\pi, 0) = 0.5$ holds, achieve the maximum ZOC. In particular, this includes the case of independent phases with uniform marginal distributions, i.e., $p(0, 0) = p(\pi, \pi) = p(0, \pi) = p(\pi, 0) = 0.25$.

The outage probability for the considered scenario with $N = 2$ and $K = 2$ is shown in Fig. 12. The curve was generated by MC simulations with $1000 \text{ slow} \times 100\,000$ fast fading samples [28]. The dashed line indicates the theoretical value of the ZOC as derived in (46). It is observed that, as expected, the outage probability is zero up to this value and then starts increasing. In contrast to the non-quantized case $K = \infty$, the outage probability is not a step function but there is an interval in which all ergodic capacities lie.

Remark 6. The above result has the following important implication. By uniformly and independently varying the phases of the RIS elements, we can obtain always positive ZOC, even in the simplest case of $N = 2$ and $K = 2$.

VII. CONCLUSION

In this work, we introduced a phase hopping scheme for RIS-assisted communication systems, which converts slow fading into artificial fast fading. We showed how this helps to significantly

improve the outage performance. In particular, a positive *zero*-outage capacity can be achieved, even if only a quantized set of possible phase values is available.

Other advantages of the proposed scheme are that it neither requires CSI at the transmitter and the RIS nor any additional communication overhead to the RIS.

A summary of the expressions for the outage probability in the various considered scenarios can be found in Tab. I. This highlights that the probability becomes a step function for our proposed phase hopping scheme and is therefore zero up to a certain transmission rate. In contrast, there always is a non-zero outage probability for the case of fixed RIS phases.

Table I
SUMMARY OF THE OUTAGE PROBABILITY EXPRESSIONS FOR STATIC AND VARYING RIS PHASES.

Scheme	Non-Line-of-Sight	Line-of-Sight
Static Phases (Section III)	$1 - \exp\left(-\frac{2^R - 1}{N}\right)$ Thm. 1, (10)	$1 - Q_1\left(\sqrt{\frac{2a^2}{N}}, \sqrt{\frac{2}{N}(2^R - 1)}\right)$ Thm. 2, (16)
Phase Hopping (Sections IV and V)	$\mathbb{1}\left(R + \frac{\exp\left(\frac{1}{N}\right) \text{Ei}\left(-\frac{1}{N}\right)}{\log 2}\right)$ Thm. 4, (28) Thm. 6	$\mathbb{1}(R - C_{\text{erg,LOS}})$ Thm. 5, (32) Thm. 6

In this work, we mostly discussed the case that the hopping of all RIS phases happens independently and uniformly distributed over the set of available phase values. For the special case of $N = 2$ and $K = 2$, it was shown in Section VI that this is an optimal strategy to maximize the ZOC. However, even though it also achieves a good performance for other N and K , it remains an open problem whether this strategy is optimal in general. This needs to be considered in future work.

In Section IV-A and Appendix B, we briefly discuss the influence of a finite number of phase hopping symbols on the outage probability ε . In particular, ε is not a perfect step function in the case of averaging over a finite number of symbols. Therefore, it will be interesting in future work to further analyze the influence of finite blocklengths on the proposed phase hopping scheme. This will particularly interesting when adding strict latency requirements, e.g., in the context of URLLC.

The results presented in this work are based on one particular channel model. Another possible extension for future work is, therefore, to consider different channel models.

APPENDIX A
PROOF OF COROLLARY 1

In order to simplify the notation, we use the shorthand $s = 2^R - 1$ in the following.

First, it can be seen from (10) in Theorem 1 that $\varepsilon_{\text{stat,NLOS}}$ is equal to the CDF of an exponential distribution. Recall, that this is equivalent to a (central) χ^2 distribution with two degrees of freedom [34, Chap. 11], i.e., a noncentral χ^2 distribution with noncentrality parameter 0 [34, Chap. 12].

Next, from Theorem 2 we can see that $\varepsilon_{\text{stat,LOS}}$ is given as the CDF of a noncentral χ^2 distribution with two degrees of freedom and noncentrality parameter $\frac{2a^2}{N}$.

With the observation that $\frac{2a^2}{N} > 0$ for $a > 0$, the statement immediately follows from [41, Thm. 3].

APPENDIX B
POSITIVE ZOC WITH FINITELY MANY SYMBOLS

Consider a NLOS phase hopping system where each transmitted symbol is repeated L times. This increases the overall channel gain of this particular symbol to

$$\sum_{l=1}^L \left| \sum_{i=1}^N \exp(j(\theta_{i,l} + \tilde{\varphi}_i)) \right|^2. \quad (47)$$

However, since we repeat the same information L times, the resulting data rate reduces by a factor of $1/L$ to

$$\frac{1}{L} \log_2 \left(1 + \sum_{l=1}^L \left| \sum_{i=1}^N \exp(j(\theta_{i,l} + \tilde{\varphi}_i)) \right|^2 \right). \quad (48)$$

Recall that the channel phases $\tilde{\varphi}_i$ are assumed to be constant for the whole transmission.

We will now show that it is possible to achieve a positive ZOC by this scheme. For this, let $N = 2$ and $L = 2$ with $\theta_{1,1} = \theta_{1,2} = 0$, $\theta_{2,1} = 0$ and $\theta_{2,2} = \pi$. The resulting channel gain from (47) is then given as

$$|\exp(j\tilde{\varphi}_1) + \exp(j\tilde{\varphi}_2)|^2 + |\exp(j\tilde{\varphi}_1) + \exp(j(\tilde{\varphi}_2 + \pi))|^2. \quad (49)$$

With the equivalence

$$|e^{j(\tilde{\varphi}_1 + \theta_1)} + e^{j(\tilde{\varphi}_2 + \theta_2)}|^2 = 2 + 2 \cos(\tilde{\varphi}_1 - \tilde{\varphi}_2 + \theta_1 - \theta_2),$$

we get that (49) is equivalent to 4, independent of $\tilde{\varphi}_1$ and $\tilde{\varphi}_2$. This yields the overall rate of

$$\frac{1}{2} \log_2 \left(1 + \sum_{l=1}^2 \left| \sum_{i=1}^2 \exp(j(\theta_{i,l} + \tilde{\varphi}_i)) \right|^2 \right) = 0.5 \log_2(5) = 1.161. \quad (50)$$

With this result, we can conclude that a positive rate is achievable, independent of the realization of $\tilde{\varphi}_1$ and $\tilde{\varphi}_2$. Therefore, also the average over a finite number of fast fading samples is positive.

REFERENCES

- [1] E. A. Jorswieck, K.-L. Besser, and C. Sun, "Artificial fast fading from reconfigurable surfaces enables ultra-reliable communications," in *2021 IEEE 22nd International Workshop on Signal Processing Advances in Wireless Communications (SPAWC)*, Lucca, Italy: IEEE, Sep. 2021.
- [2] M. D. Renzo, A. Zappone, M. Debbah, M. S. Alouini, C. Yuen, J. D. Rosny, and S. Tretyakov, "Smart radio environments empowered by reconfigurable intelligent surfaces: How it works, state of research, and road ahead," *IEEE Journal on Selected Areas in Communications*, vol. 38, no. 11, pp. 2450–2525, 2020. DOI: [10.1109/JSAC.2020.3007211](https://doi.org/10.1109/JSAC.2020.3007211). arXiv: [2004.09352](https://arxiv.org/abs/2004.09352) [cs.IT].
- [3] E. Björnson and L. Sanguinetti, "Power scaling laws and near-field behaviors of massive MIMO and intelligent reflecting surfaces," *IEEE Open Journal of the Communications Society*, vol. 1, pp. 1306–1324, 2020. DOI: [10.1109/OJCOMS.2020.3020925](https://doi.org/10.1109/OJCOMS.2020.3020925).
- [4] M. A. ElMossallamy, H. Zhang, L. Song, K. G. Seddik, Z. Han, and G. Y. Li, "Reconfigurable intelligent surfaces for wireless communications: Principles, challenges, and opportunities," *IEEE Transactions on Cognitive Communications and Networking*, vol. 6, no. 3, pp. 990–1002, 2020. DOI: [10.1109/TCCN.2020.2992604](https://doi.org/10.1109/TCCN.2020.2992604).
- [5] N. Kaina, M. Dupré, G. Lerosey, and M. Fink, "Shaping complex microwave fields in reverberating media with binary tunable metasurfaces," *Scientific Reports*, vol. 4, no. 1, Oct. 2014. DOI: [10.1038/srep06693](https://doi.org/10.1038/srep06693).
- [6] P. del Hougne, M. Fink, and G. Lerosey, "Optimally diverse communication channels in disordered environments with tuned randomness," *Nature Electronics*, vol. 2, no. 1, pp. 36–41, Jan. 2019. DOI: [10.1038/s41928-018-0190-1](https://doi.org/10.1038/s41928-018-0190-1).
- [7] E. Basar, "Reconfigurable intelligent surfaces for doppler effect and multipath fading mitigation," *Frontiers in Communications and Networks*, vol. 2, May 2021. DOI: [10.3389/frcmn.2021.672857](https://doi.org/10.3389/frcmn.2021.672857). arXiv: [1912.04080](https://arxiv.org/abs/1912.04080) [eess.SP].
- [8] Z. Huang, B. Zheng, and R. Zhang, "Transforming fading channel from fast to slow: IRS-assisted high-mobility communication," in *ICC 2021 – 2021 IEEE International Conference on Communications (ICC)*, Montreal, QC, Canada: IEEE, Jun. 2021. arXiv: [2011.03147](https://arxiv.org/abs/2011.03147) [cs.IT].
- [9] E. Björnson, H. Wymeersch, B. Matthiesen, P. Popovski, L. Sanguinetti, and E. de Carvalho, *Reconfigurable intelligent surfaces: A signal processing perspective with wireless applications*, Feb. 2021. arXiv: [2102.00742](https://arxiv.org/abs/2102.00742) [eess.SP].
- [10] H. Wymeersch, J. He, B. Denis, A. Clemente, and M. Juntti, "Radio localization and mapping with reconfigurable intelligent surfaces: Challenges, opportunities, and research directions," *IEEE Vehicular Technology Magazine*, vol. 15, no. 4, pp. 52–61, Dec. 2020. DOI: [10.1109/mvt.2020.3023682](https://doi.org/10.1109/mvt.2020.3023682).
- [11] Q. Wu and R. Zhang, "Intelligent reflecting surface enhanced wireless network via joint active and passive beamforming," *IEEE Transactions on Wireless Communications*, vol. 18, no. 11, pp. 5394–5409, 2019. DOI: [10.1109/TWC.2019.2936025](https://doi.org/10.1109/TWC.2019.2936025).
- [12] S. Abeywickrama, R. Zhang, Q. Wu, and C. Yuen, "Intelligent reflecting surface: Practical phase shift model and beamforming optimization," *IEEE Transactions on Communications*, vol. 68, no. 9, pp. 5849–5863, Sep. 2020. DOI: [10.1109/TCOMM.2020.3001125](https://doi.org/10.1109/TCOMM.2020.3001125). arXiv: [2002.10112](https://arxiv.org/abs/2002.10112) [cs.IT].

- [13] C. Huang, A. Zappone, G. C. Alexandropoulos, M. Debbah, and C. Yuen, “Reconfigurable intelligent surfaces for energy efficiency in wireless communication,” *IEEE Transactions on Wireless Communications*, vol. 18, no. 8, pp. 4157–4170, Aug. 2019. DOI: [10.1109/twc.2019.2922609](https://doi.org/10.1109/twc.2019.2922609). arXiv: [1810.06934](https://arxiv.org/abs/1810.06934) [cs.IT].
- [14] X. Liu, C. Sun, and E. A. Jorswieck, “Two-user SINR region for reconfigurable intelligent surface aided downlink channel,” in *2021 IEEE International Conference on Communications Workshops (ICC Workshops)*, IEEE, Jun. 2021. DOI: [10.1109/iccworkshops50388.2021.9473858](https://doi.org/10.1109/iccworkshops50388.2021.9473858).
- [15] E. Björnson, Ö. Özdogan, and E. G. Larsson, “Intelligent reflecting surface versus decode-and-forward: How large surfaces are needed to beat relaying?” *IEEE Wireless Communications Letters*, vol. 9, no. 2, pp. 244–248, Feb. 2020. DOI: [10.1109/LWC.2019.2950624](https://doi.org/10.1109/LWC.2019.2950624). arXiv: [1906.03949](https://arxiv.org/abs/1906.03949) [cs.IT].
- [16] M. Dunna, C. Zhang, D. Sievenpiper, and D. Bharadia, “ScatterMIMO: Enabling virtual MIMO with smart surfaces,” in *Proceedings of the 26th Annual International Conference on Mobile Computing and Networking*, ser. MobiCom '20, London, United Kingdom: Association for Computing Machinery, Apr. 2020. DOI: [10.1145/3372224.3380887](https://doi.org/10.1145/3372224.3380887).
- [17] D. Torrieri, *Principles of Spread-Spectrum Communication Systems*. Springer International Publishing, 2018. DOI: [10.1007/978-3-319-70569-9](https://doi.org/10.1007/978-3-319-70569-9).
- [18] M.-M. Zhao, Q. Wu, M.-J. Zhao, and R. Zhang, “Intelligent reflecting surface enhanced wireless networks: Two-timescale beamforming optimization,” *IEEE Transactions on Wireless Communications*, vol. 20, no. 1, pp. 2–17, Jan. 2021. DOI: [10.1109/twc.2020.3022297](https://doi.org/10.1109/twc.2020.3022297).
- [19] K. Zhi, C. Pan, H. Ren, and K. Wang, “Statistical CSI-based design for reconfigurable intelligent surface-aided massive MIMO systems with direct links,” *IEEE Wireless Communications Letters*, vol. 10, no. 5, pp. 1128–1132, May 2021. DOI: [10.1109/LWC.2021.3059938](https://doi.org/10.1109/LWC.2021.3059938).
- [20] K. Zhi, C. Pan, H. Ren, and K. Wang, *Ergodic rate analysis of reconfigurable intelligent surface-aided massive MIMO systems with ZF detectors*, Jul. 2021. arXiv: [2107.07925](https://arxiv.org/abs/2107.07925) [cs.IT].
- [21] J. P. Turpin, J. A. Bossard, K. L. Morgan, D. H. Werner, and P. L. Werner, “Reconfigurable and tunable metamaterials: A review of the theory and applications,” *International Journal of Antennas and Propagation*, vol. 2014, pp. 1–18, 2014. DOI: [10.1155/2014/429837](https://doi.org/10.1155/2014/429837).
- [22] B. O. Zhu, J. Zhao, and Y. Feng, “Active impedance metasurface with full 360° reflection phase tuning,” *Scientific Reports*, vol. 3, no. 1, p. 3059, Nov. 2013. DOI: [10.1038/srep03059](https://doi.org/10.1038/srep03059).
- [23] R. Fara, P. Ratajczak, D.-T. Phan-Huy, A. Ourir, M. Di Renzo, and J. De Rosny, *A prototype of reconfigurable intelligent surface with continuous control of the reflection phase*, May 2021. arXiv: [2105.11862](https://arxiv.org/abs/2105.11862) [eess.SP].
- [24] N. Kaina, M. Dupré, M. Fink, and G. Lerosey, “Hybridized resonances to design tunable binary phase metasurface unit cells,” *Optics Express*, vol. 22, no. 16, p. 18 881, Jul. 2014. DOI: [10.1364/OE.22.018881](https://doi.org/10.1364/OE.22.018881).
- [25] Q. Wu and R. Zhang, “Beamforming optimization for wireless network aided by intelligent reflecting surface with discrete phase shifts,” *IEEE Transactions on Communications*, vol. 68, no. 3, pp. 1838–1851, Mar. 2020. DOI: [10.1109/TCOMM.2019.2958916](https://doi.org/10.1109/TCOMM.2019.2958916). arXiv: [1906.03165](https://arxiv.org/abs/1906.03165) [cs.IT].
- [26] H. Zhang, B. Di, L. Song, and Z. Han, “Reconfigurable intelligent surfaces assisted communications with limited phase shifts: How many phase shifts are enough?” *IEEE Transactions on Vehicular Technology*, vol. 69, no. 4, pp. 4498–4502, Apr. 2020. DOI: [10.1109/TVT.2020.2973073](https://doi.org/10.1109/TVT.2020.2973073). arXiv: [1912.01477](https://arxiv.org/abs/1912.01477) [cs.IT].
- [27] T. Wang, G. Chen, J. P. Coon, and M.-A. Badiu, “Study of intelligent reflective surface assisted communications with one-bit phase adjustments,” in *GLOBECOM 2020 – 2020 IEEE Global Communications Conference*, Taipei, Taiwan: IEEE, Dec. 2020. DOI: [10.1109/GLOBECOM42002.2020.9322575](https://doi.org/10.1109/GLOBECOM42002.2020.9322575). arXiv: [2008.09770](https://arxiv.org/abs/2008.09770) [eess.SP].
- [28] K.-L. Besser. (2021). “Artificial fast fading from RIS, Supplementary material,” [Online]. Available: <https://gitlab.com/klb2/ris-phase-hopping>.

- [29] J. He, H. Wymeersch, T. Sanguanpuak, O. Silven, and M. Juntti, "Adaptive beamforming design for mmWave RIS-aided joint localization and communication," in *2020 IEEE Wireless Communications and Networking Conference Workshops (WCNCW)*, 2020. DOI: [10.1109/WCNCW48565.2020.9124848](https://doi.org/10.1109/WCNCW48565.2020.9124848).
- [30] J. M. Romero-Jerez, F. J. Lopez-Martinez, J. F. Paris, and A. J. Goldsmith, "The fluctuating two-ray fading model: Statistical characterization and performance analysis," *IEEE Transactions on Wireless Communications*, vol. 16, no. 7, pp. 4420–4432, 2017. DOI: [10.1109/TWC.2017.2698445](https://doi.org/10.1109/TWC.2017.2698445).
- [31] D. Tse and P. Viswanath, *Fundamentals of Wireless Communications*. Cambridge University Press, 2005.
- [32] S. R. Jammalamadaka and A. SenGupta, *Topics in Circular Statistics*, ser. Series on Multivariate Analysis. World Scientific, 2001, vol. 5. DOI: [10.1142/4031](https://doi.org/10.1142/4031).
- [33] N. M. Temme, "Asymptotic and numerical aspects of the noncentral chi-square distribution," *Computers and Mathematics with Applications*, vol. 25, no. 5, pp. 55–63, Mar. 1993. DOI: [10.1016/0898-1221\(93\)90198-5](https://doi.org/10.1016/0898-1221(93)90198-5).
- [34] C. Forbes, M. Evans, N. Hastings, and B. Peacock, *Statistical Distributions*, 4th ed. John Wiley & Sons, Inc., 2010.
- [35] R. Ezzine, W. Labidi, H. Boche, and C. Deppe, "Common randomness generation and identification over gaussian channels," in *GLOBECOM 2020 - 2020 IEEE Global Communications Conference*, Taipei, Taiwan: IEEE, Dec. 2020. DOI: [10.1109/globecom42002.2020.9322460](https://doi.org/10.1109/globecom42002.2020.9322460).
- [36] A. D. Poularikas, Ed., *Transforms and Applications Handbook*, 3rd ed., ser. The Electrical Engineering Handbook Series. CRC Press, 2010. DOI: [10.1201/9781315218915](https://doi.org/10.1201/9781315218915).
- [37] H. Ogata, "A numerical integration formula based on the Bessel functions," *Publications of the Research Institute for Mathematical Sciences*, vol. 41, no. 4, pp. 949–970, 2005. DOI: [10.2977/prims/1145474602](https://doi.org/10.2977/prims/1145474602).
- [38] S. Murray and F. Poulin, "Hankel: A Python library for performing simple and accurate Hankel transformations," *Journal of Open Source Software*, vol. 4, no. 37, p. 1397, May 2019. DOI: [10.21105/joss.01397](https://doi.org/10.21105/joss.01397).
- [39] M. Abramowitz and I. A. Stegun, *Handbook of Mathematical Functions: With Formulas, Graphs, and Mathematical Tables*, 10th Ed. 1972.
- [40] K.-L. Besser, P.-H. Lin, and E. A. Jorswieck, "On fading channel dependency structures with a positive zero-outage capacity," *IEEE Transactions to Communications*, 2021. DOI: [10.1109/TCOMM.2021.3097755](https://doi.org/10.1109/TCOMM.2021.3097755). arXiv: [2102.02541 \[cs.IT\]](https://arxiv.org/abs/2102.02541), Early Access.
- [41] T. Mathew and K. Nordström, "Inequalities for the probability content of a rotated ellipse and related stochastic domination results," *The Annals of Applied Probability*, vol. 7, no. 4, pp. 1106–1117, Nov. 1997. DOI: [10.1214/aoap/1043862426](https://doi.org/10.1214/aoap/1043862426).